

Cite this: *New J. Chem.*, 2012, **36**, 2630–2641

www.rsc.org/njc

PAPER

# Aluminium(III) porphyrin based axial-bonding type dyads containing thiaporphyrins and expanded thiaporphyrins as axial ligands†

Avijit Ghosh,<sup>a</sup> Dilip Kumar Maity<sup>\*b</sup> and Mangalampalli Ravikanth<sup>\*a</sup>

Received (in Montpellier, France) 20th July 2012, Accepted 27th September 2012

DOI: 10.1039/c2nj40631d

Four axial-bonding type Al(III) porphyrin based dyads, containing thiaporphyrins with N<sub>3</sub>S **1** and N<sub>2</sub>S<sub>2</sub> **2** cores and expanded thiaporphyrins with N<sub>2</sub>S<sub>3</sub> **3** and N<sub>2</sub>S<sub>4</sub> **4** cores, were synthesised by treating [(TPP)Al<sup>III</sup>OH] with the corresponding mono-functionalised *meso*-4-hydroxyphenyl thiaporphyrin or expanded thiaporphyrin building blocks in benzene at refluxing temperature. The stable dyads **1–4** are freely soluble in common organic solvents and characterized by mass, 1D and 2D NMR, absorption, electrochemical and fluorescence techniques. 1D and 2D NMR studies unambiguously confirmed the dyads. The absorption and electrochemical studies show weak interaction between the two macrocycles in dyads and the constituted macrocycles in dyads mostly retain their characteristic individual features. The steady state fluorescence studies indicate a decrease in the quantum yield of Al(III) porphyrin unit in dyads **1–4** and invoked the possibility of singlet–singlet energy transfer from the Al(III) porphyrin unit to the N<sub>3</sub>S porphyrin unit in dyad **1** and N<sub>2</sub>S<sub>2</sub> porphyrin unit in dyad **2**. Structural information of these dyads in their ground (S<sub>0</sub>) state are generated by applying density functional theory (DFT) based quantum chemical calculations. Excited state calculations are carried out following time dependent density functional theory (TD-DFT) and UV-Vis spectra of these dyads are simulated in the Soret band region.

## Introduction

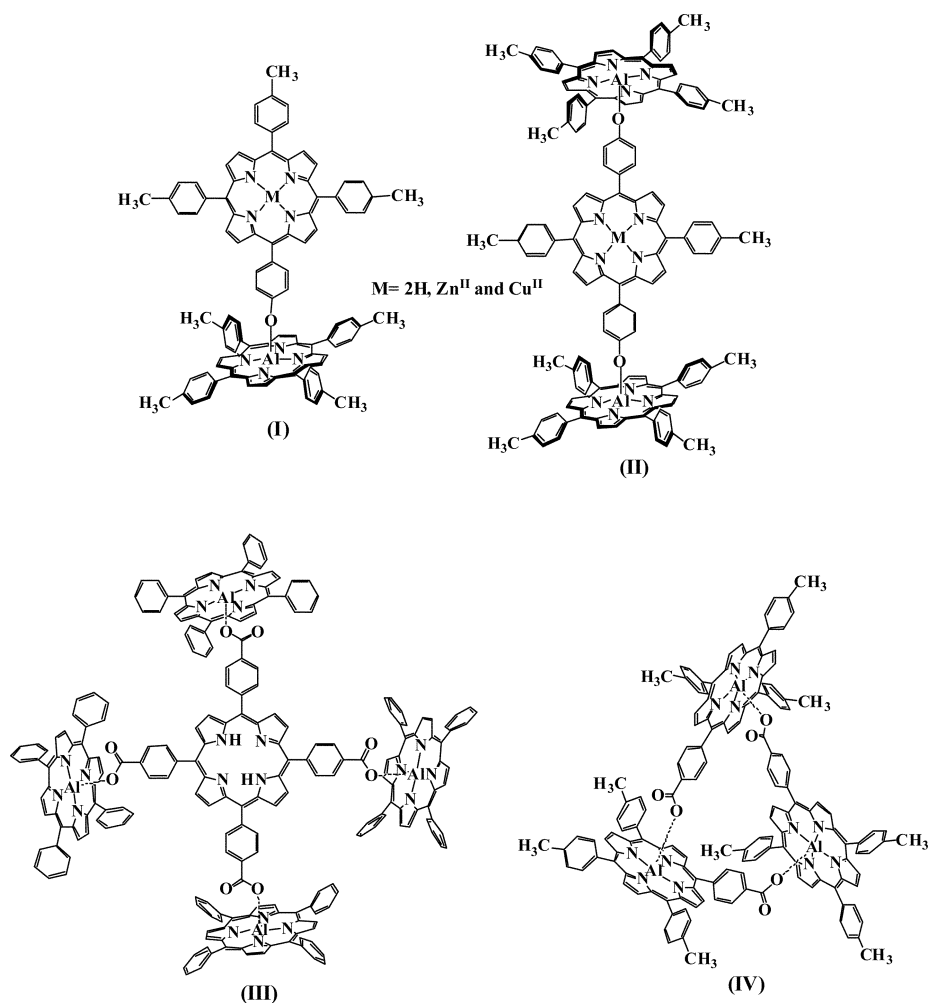
Multiporphyrin arrays have been an area of intense research because of their use in various research fields, such as molecular recognition, sensing, molecular-level electronics and mimics natural systems.<sup>1</sup> Multiporphyrins have been assembled by either covalent<sup>2</sup> or non-covalent<sup>3</sup> interactions such as hydrogen bonding, coordination bonding, stacking interactions *etc.* However, designing and building arrays utilizing axial coordination has proven to be a useful approach for the development of these assemblies with well defined geometries.<sup>4</sup> The axial-bonding approach is very flexible and conveniently employed for the design and synthesis of more elaborate, hybrid type porphyrin arrays with diverse structures and functions. For example, photochemically active, main group element-containing porphyrins as the basal scaffold unit and free base porphyrins, metalloporphyrins or metalloid porphyrins as the axial donor/acceptor units are required for the construction of multiporphyrin arrays with varying spectral, redox and photophysical properties. Thus, the knowledge of the preferred coordination

number, geometry and ligand preference of a metalloporphyrin allows for the rational design of multiporphyrin arrays. Maiya,<sup>4</sup> Sanders<sup>4</sup> and others<sup>5</sup> have used the axial-bonding approach to construct several interesting hybrid type multiporphyrin arrays by using main-group elements or metalloid-containing porphyrins as a basal scaffold. However, the reports on ‘axial-bonding’ arrays are still limited although different porphyrins and related macrocycles, such as corroles and expanded porphyrins, which can be used as axial ligands, are readily available by simple synthetic methodologies. The literature reports on axial-bonding porphyrin arrays are mainly based on phosphorus(v),<sup>4a,f–h,5f</sup> tin(iv),<sup>4e,g,k–m,5a–d</sup> and germanium(iv)<sup>4g</sup> porphyrins, with the majority of them having been constructed by utilizing the oxophilicity of the central metalloid ion. Aluminium(III) porphyrins are known to possess rich redox and photochemical activities<sup>6</sup> and the well-known strength of the Al–O bond can be efficiently utilized to build functionally active molecular arrays. Although Al(III) ion is also oxophilic, the reports on the axial-bonding type of porphyrin arrays using Al(III) porphyrin as a basal scaffold unit are very few<sup>7</sup> (Scheme 1). For many years, Al(III) porphyrins have been used as a catalyst for various organic transformations.<sup>8</sup> Kumar and Maiya<sup>7a</sup> reported the first examples of Al(III) porphyrin based axial-bonding type dyads and triads (Scheme 1; compound I & II) by reacting hydroxy Al(III) porphyrin<sup>9</sup> (**5**) with an excess of free base porphyrin containing one *meso*-hydroxyphenyl group. The metallation, spectral, electrochemical and photophysical

<sup>a</sup> Department of Chemistry, Indian Institute of Technology Bombay, Powai, Mumbai 400 076, India. E-mail: ravikanth@chem.iitb.ac.in; Fax: +91-22-25767152; Tel: +91-22-25767176

<sup>b</sup> Theoretical Chemistry Section, Chemistry Group, Bhabha Atomic Research Centre, Mumbai 400085, India. E-mail: dkmaity@barc.gov.in

† Electronic supplementary information (ESI) available. See DOI: 10.1039/c2nj40631d



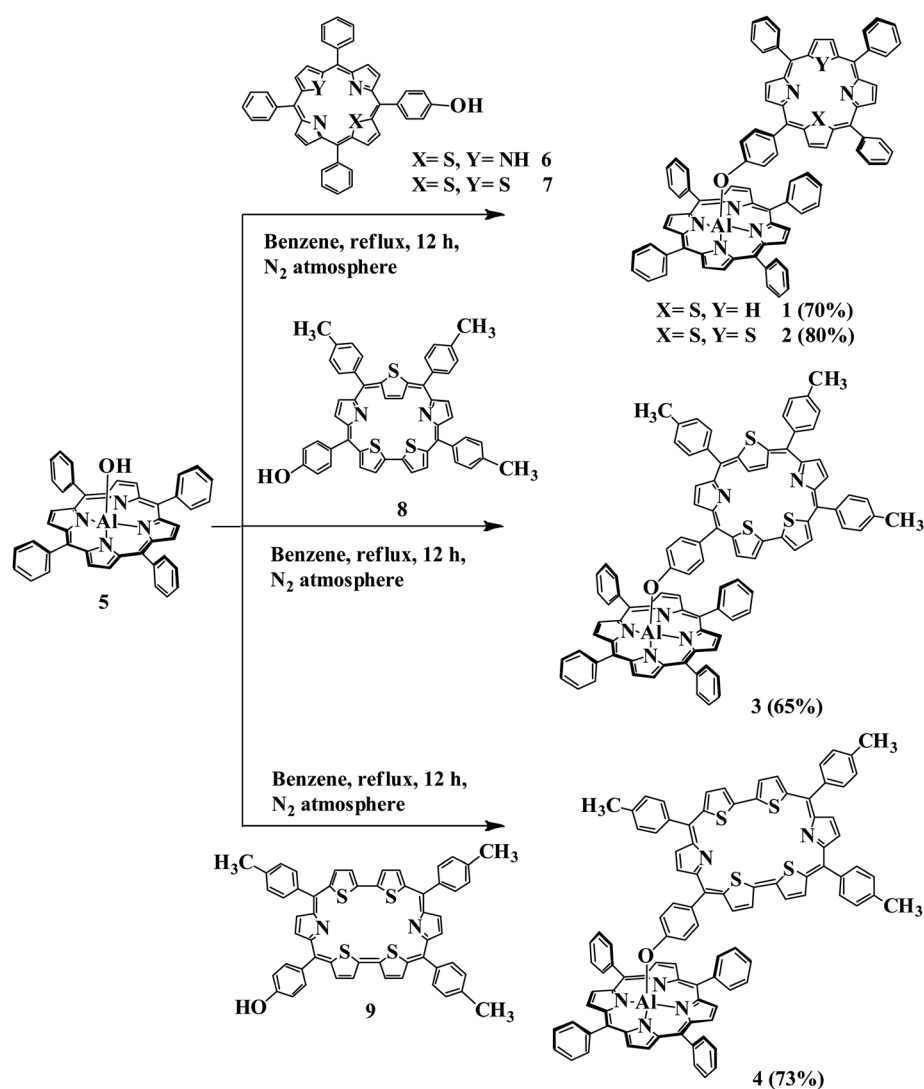
**Scheme 1** Al(III) porphyrin based 'axial-bonding type' multiporphyrin arrays.

properties of Al(III) porphyrin based dyads and triads were also explored. Sanders and co-workers<sup>7b</sup> reported the synthesis of a porphyrin pentad containing one central tetra(4-carboxyphenyl)-porphyrin surrounded by four Al(III) tetraphenylporphyrins (Scheme 1; compound III). Sanders and co-workers<sup>7c</sup> also reported the synthesis of a cyclic triad (Scheme 1; compound IV) using Al(III) porphyrin containing a *meso*-carboxyphenyl group by a self-assembly process. To the best of our knowledge, there is no report on axial-bonding type Al(III) porphyrin based dyads or higher oligomers in which thiaporphyrins or expanded thiaporphyrins have been used as axial ligands. Thiaporphyrins result from the replacement of one or two pyrrole moieties with thiophene rings ( $N_3S$  or  $N_2S_2$  core) and possess very interesting physico-chemical properties, which are quite different from normal porphyrins<sup>10</sup> ( $N_4$  core). Expanded thiaporphyrins containing more than four heterocyclic rings, such as a combination of pyrroles and thiophenes connected by methine bridges or directly, and possess very different properties from regular porphyrins due to their large cavity size and more  $\pi$ -electrons.<sup>11</sup> In this paper, we report the synthesis of the first examples of stable axial-bonding type dyads **1–4** (Scheme 2) in which Al(III) porphyrin is used as the basal porphyrin and thiaporphyrins with  $N_3S$  and  $N_2S_2$  cores as well as expanded thiaporphyrins, such as thiasapphyrin with a  $N_2S_3$  core and

thiarubyrin with a  $N_2S_4$  core, are used as axial ligands (Scheme 2). The spectral, electrochemical and photophysical properties of these novel Al(III) porphyrin based axial bonding type unsymmetrical porphyrin dyads containing two different macrocycles are also described. The structures of these four multiporphyrin dyads are predicted by applying density functional theory (DFT) based electronic structure calculations adopting all electron Gaussian atomic basis functions. Excited state calculations are carried out following time dependent density functional theory (TD-DFT) to assign electronic transitions involved in these four dyads and to simulate UV-Vis spectra in the Soret band region.

## Results and discussion

The required mono-functionalized thiaporphyrin/expanded thiaporphyrin building blocks containing one *meso*-hydroxyphenyl group **5–8** (Scheme 2) were synthesised in decent yields by slight modification of available literature procedures<sup>12</sup> (S14–S16, ESI†). The dyads **1–4** were prepared by refluxing one equivalent of  $[(TPP)Al^{III}OH]^9$  with one equivalent of corresponding thiaporphyrin (**5/6**) or expanded thiaporphyrin (**7/8**) in benzene at refluxing temperature for 12 h (Scheme 2). The progress of these reactions were followed by alumina TLC analysis since the products readily decomposes on silica TLC.



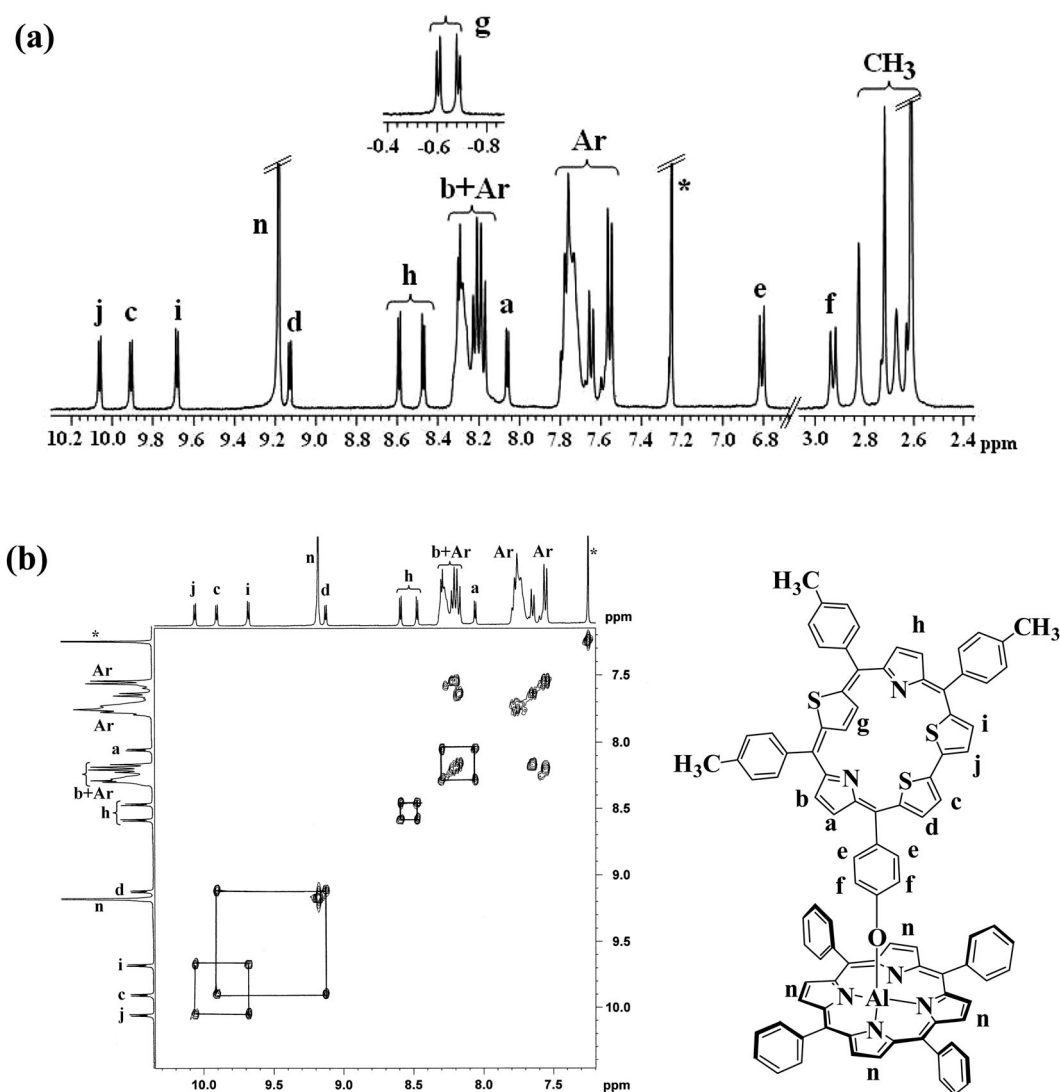
**Scheme 2** Synthesis of four Al(III) porphyrin based 'axial-bonding type' dyads **1–4**.

Furthermore, as the reaction advances, the colour of the reaction mixture darkens, indicating the progress of the reaction. The crude reaction mixture after standard work-up was subjected to neutral alumina column chromatographic purification and afforded dyads **1** and **2** as red solids and dyads **3** and **4** as dark purple solids in very good yields (60–80%). The dyads are freely soluble in common organic solvents and characterized by elemental analysis, MALDI-TOF mass, 1D and 2D NMR, absorption, electrochemical and fluorescence techniques. The MALDI-mass spectra (S3–S6, ESI<sup>+</sup>) showed molecular ion peak and the elemental analyses matched closely with the expected composition of dyads, confirming the identity of the dyads **1–4**.

## NMR studies

Detailed NMR studies were carried out to unambiguously confirm the formation of dyads **1–4**. The <sup>1</sup>H NMR spectra along with its <sup>1</sup>H–<sup>1</sup>H COSY spectra for dyad **3** are presented in Fig. 1. NMR data of selected protons of axial thiaporphyrin/expanded thiaporphyrin unit in dyads **1–4**, which showed clear

changes in their chemical shifts on dyad formation, are presented in Table 1. The <sup>1</sup>H NMR spectra were analyzed on the basis of the resonance position and integrated intensity data, as well as the proton-to-proton connectivity information revealed in the COSY spectra, to arrive at the structures of these new compounds. We used <sup>1</sup>H–<sup>1</sup>H COSY NMR to identify the β-pyrrole, β-thiophene and bridging phenoxo protons of axial thiaporphyrin/expanded thiaporphyrin unit, as shown in Fig. 1b for dyad **3**. In dyad **3**, the four β-thiophene protons of the bithiophene moiety of the axial thiasapphyrin unit appeared as four sets of doublets at 10.05, 9.90, 9.68 and 9.12 ppm. Among these, the doublet at 10.05 ppm showed cross peak connectivity with the doublet at 9.68 ppm and the doublet at 9.90 ppm showed cross peak connectivity with the doublet at 9.12 ppm, as revealed in the <sup>1</sup>H–<sup>1</sup>H COSY spectrum (Fig. 1b). Thus, the signals at 9.90 and 9.12 ppm were assigned as type c and type d protons of bithiophene, respectively. The doublets at 10.05 and 9.68 ppm were due to type i and type j protons of bithiophene, respectively. Furthermore, in dyad **3**, the thiophene ring which is opposite to the bithiophene moiety remains inverted, like in the corresponding thiasapphyrin monomer

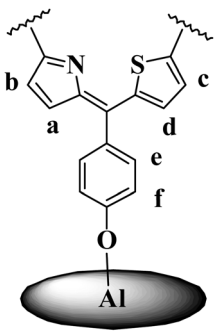


**Fig. 1** (a)  $^1\text{H}$  NMR and (b) partial  $^1\text{H}$ - $^1\text{H}$  COSY spectra of dyad **3** recorded in  $\text{CDCl}_3$  at room temperature. The inset in (a) shows the signal for inverted thiophene.

**8** and these protons (type g) appeared as two doublets at  $-0.61$  and  $-0.69$  ppm. The four  $\beta$ -pyrrole protons of the axial thiasapphyrin unit, represented as type a, b and h, appeared as four sets of doublets at 8.05, 8.25 (merged into the multiplet signal of aromatic protons), 8.47 and 8.59 ppm. Based on correlations in the COSY NMR, we identified doublets at 8.05 and 8.25 ppm as type a and type b pyrrole protons, respectively. The other two doublets at 8.47 and 8.59 ppm were due to type h pyrrole protons. As is clear from Fig. 1 and the data presented in Table 1, only certain protons of the axial thiaporphyrin/expanded thiaporphyrin unit, which fall in the ring current effect of the basal  $\text{Al}(\text{III})$  porphyrin unit, experience upfield shifts and all other protons of both axial and basal units exhibit negligible shifts compared to their reference monomers. For example, in dyad **3** containing thiasapphyrin as the axial ligand, the pyrrole (type a and b) and thiophene (type c and d) protons of the axial ligand that fall in the ring current effect of  $\text{Al}(\text{III})$  porphyrin were upfield shifted by 0.2–0.6 ppm compared to the thiasapphyrin monomer **8**. The other  $\beta$ -pyrrole as well as  $\beta$ -thiophene protons that were not facing the basal  $\text{Al}(\text{III})$  porphyrin did not exhibit

much change in their chemical shifts. Similarly, the  $\beta$ -pyrrole protons of  $\text{Al}(\text{III})$  porphyrins also did not exhibit much change in their chemical shifts on dyad formation. In fact the eight  $\beta$ -pyrrole protons of  $\text{Al}(\text{III})$  porphyrin appeared as a sharp singlet, though we expect a greater number of signals based on the DFT optimized structures, which showed an asymmetrical environment for pyrrole protons. The  $^1\text{H}$  NMR recorded for dyad **2** at  $-40^\circ\text{C}$  showed the splitting of the singlet signal of eight  $\beta$ -pyrrole protons of basal  $\text{Al}(\text{III})$  porphyrin into two broad signals, indicating that the  $\beta$ -pyrrole protons can appear as a greater number of signals with decrease of temperature (S12, ESI $^\dagger$ ). Since we observed only a single resonance for the eight  $\beta$ -pyrrole protons of the basal  $\text{Al}(\text{III})$  porphyrin at room temperature, this supports the fast rotation along the  $\text{Al}-\text{O}$  bond, resulting in a symmetrical environment of all  $\beta$ -pyrrole protons. However, the most prominent change in the chemical shifts was noted for the bridging phenoxo group of thiasapphyrin that is bound to the  $\text{Al}(\text{III})$  center. The protons on the phenoxo bridge (type e and f) simultaneously exhibit the shielding effect of the basal  $\text{Al}(\text{III})$  porphyrin and the deshielding effect of the axial thiasapphyrin.

**Table 1**  $^1\text{H}$  NMR data of selected protons of dyads **1–4** recorded in  $\text{CDCl}_3$ 

 <p style="text-align: center;"><b>Dyad</b></p>						
Axial unit						
	$\beta$ -Pyrrole		$\beta$ -Thiophene		Bridging phenyl	
Compound	a	b	c	d	e	f
<b>1</b>	8.15 (m) <sup>a</sup>	8.36 (d)	9.47 (d)	9.18 (d)	6.74 (d)	2.88 (d)
<b>2</b>	8.09 (d)	8.43 (d)	9.41 (d)	9.09 (d)	6.73 (d)	2.89 (d)
<b>3</b>	8.05 (d)	8.25 (m) <sup>a</sup>	9.90 (d)	9.12 (d)	6.80 (d)	2.91 (d)
<b>4</b>	8.35 (m) <sup>a</sup>	8.77 (d)	11.24 (d)	9.76 (d)	7.04 (d)	3.06 (d)

<sup>a</sup> Overlapped with the aryl protons and appeared along with the multiplet of aryl protons.

While the protons *meta* to the oxo group of the bridging phenyl (type e) resonate at 6.80 ppm, those *ortho* to the oxo group (type f), which are closer to the Al(III) porphyrin, experience more ring current effect and resonate at 2.91 ppm, which clearly reflects the proton–proton connectivity pattern in the  $^1\text{H}$ – $^1\text{H}$  COSY spectrum (S7, ESI<sup>†</sup>). The same protons of the phenoxo group (type e and f) in its corresponding sapphyrin monomer **8** appear as a multiplet at  $\sim 7.15$  ppm. Thus, the NMR spectral shifts clearly confirm the formation of dyad **3**. The dyads **1**, **2** and **4** also showed similar NMR features to dyad **3**, confirming their formation (S8–S14, ESI<sup>†</sup>).

### Spectral and electrochemical properties

The absorption spectra of dyads **1** and **3** along with their corresponding 1 : 1 mixture of monomers recorded in dichloromethane are shown in Fig. 2 and the data are tabulated in Table 2. As is clear from Fig. 2 and the data in Table 2, the absorption spectra of dyads **1–4** appear to be nearly a superimposition of the spectra of the corresponding constituted monomers with negligible shifts in their peak maxima. For example, the absorption spectrum of dyad **2** showed bands at 415, 436, 515, 547, 585, 635 and 698 nm, respectively, corresponding to both the constituted porphyrin units, Al(III) porphyrin and 21,23-dithiaporphyrin. Specifically, the bands at 415, 547 and 585 nm are mainly due to Al(III) porphyrin and the bands at 436, 515, 635 and 698 nm are due to the axial 21, 23-dithiaporphyrin. Similarly, the dyad **3** showed absorption bands at 415, 510, 585, 630, 686 and 887 nm, respectively, corresponding to both Al(III) porphyrin and sapphyrin units. The other dyads **1** and **4** also showed identical absorption

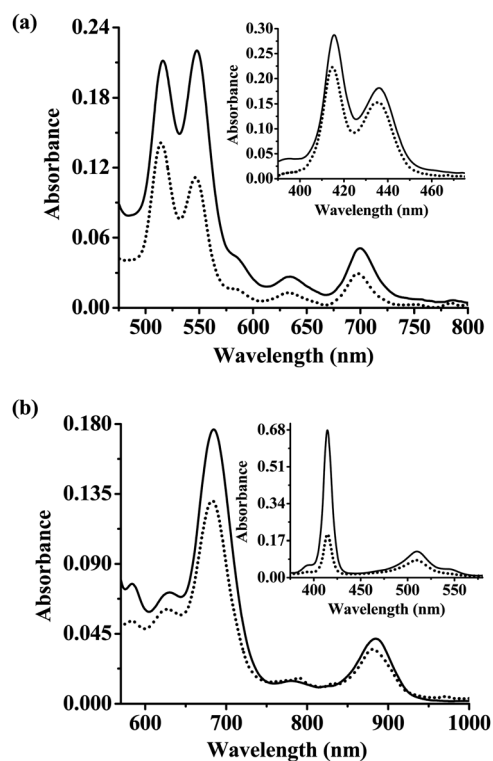


**Fig. 2** Q-band absorption spectra of (a) dyad **2** (solid line) and 1 : 1 mixture (dotted line) of corresponding constituted monomers **5** & **7** and (b) dyad **3** (solid line) and 1 : 1 mixture (dotted line) of corresponding constituted monomers **5** & **8** recorded in dichloromethane. The inset shows the corresponding Soret band absorption spectra. Concentrations of solution used for Soret band are  $1 \times 10^{-6}$  M and for Q-bands  $1 \times 10^{-5}$  M.

features (S15–S16, ESI<sup>†</sup>). However, the extinction coefficients of the absorption bands of the dyads are significantly higher compared to their 1 : 1 mixture of constituted monomers (Fig. 2). Thus, the absorption study revealed that dyads **1–4** showed the features of their constituted components but exhibit large changes in extinction coefficients as compared to their 1 : 1 physical mixture of corresponding monomers.

The electrochemical studies were carried out on dyads **1–4**, along with their corresponding monomers, in  $\text{CH}_2\text{Cl}_2$  using tetrabutylammonium perchlorate as the supporting electrolyte and the data are presented in Table 3. The oxidation and reduction waves of dyad **2** along with its constituted monomers are shown in Fig. 3. Generally, the dyads **1–4** exhibit two oxidations and two or three reductions. The reductions are reversible/quasi-reversible whereas the oxidations are irreversible and the redox potentials were easily assigned on the basis of the electrochemical data of their corresponding monomers (Table 3). The data in Table 3 and Fig. 3 clearly indicate that the redox potentials of dyads **1–4** were in the same range as those of their corresponding monomers. For example, dyad **2** containing Al(III) porphyrin and 21,23-dithiaporphyrin exhibits three oxidations at 1.00, 1.24 and 1.51 V and three reductions at  $-0.96$ ,  $-1.24$  and  $-1.51$  V. The first oxidation at 1.00 V and last reduction at  $-1.51$  V were due to the Al(III) porphyrin component; the reduction at  $-0.96$  V was exclusively due to the  $\text{N}_2\text{S}_2$  porphyrin component and the oxidation at 1.24 V and



**Table 2** Absorption data of dyads **1–4** and their corresponding 1 : 1 mixture of monomers recorded in dichloromethane

Absorption data		
Compound	Soret band $\lambda$ (nm) (log $\epsilon$ )	Q-bands $\lambda$ (nm) (log $\epsilon$ )
<b>5</b>	415 (5.42)	548 (4.03); 587 (3.29)
<b>6</b>	430 (5.17)	515 (4.15); 551 (3.78); 618 (3.31); 679 (3.48)
<b>1</b>	415 (5.72) 431 (5.31)	515 (4.24); 548 (4.37); 585 (3.60); 619 (3.43); 680 (3.61)
<b>1</b> (1 : 1) <sup>a</sup>	415 (5.35) 429 (5.01)	515 (3.96); 548 (3.90); 585 (3.15); 619 (3.15); 678 (3.30)
<b>7</b>	437 (5.23)	516 (4.22); 550 (4.01); 635 (3.19); 699 (3.58)
<b>2</b>	415 (5.45) 436 (5.26)	515 (4.32); 547 (4.34); 585 (3.63); 635 (3.42); 698 (3.70)
<b>2</b> (1 : 1) <sup>b</sup>	415 (5.35) 437 (5.17)	515 (4.15); 547 (4.04); 585 (3.20); 635 (3.10); 698 (3.46)
<b>8</b>	509 (5.03)	625 (3.74); 682 (4.16); 882 (3.55)
<b>3</b>	415 (5.82) 510 (5.08)	545 (sh); 585 (3.88); 630 (3.85); 686 (4.24); 887 (3.61)
<b>3</b> (1 : 1) <sup>c</sup>	415 (5.29) 510 (4.90)	585 (3.72); 630 (3.78); 686 (4.11); 883 (3.54)
<b>9</b>	524 (5.30)	615 (3.59); 662 (3.79); 720 (4.26); 843 (3.33); 960 (3.20)
<b>4</b>	415 (5.76) 525 (5.54)	583 (4.02); 615 (3.92); 663 (4.17); 723 (4.66); 844 (3.58); 962 (3.72)
<b>4</b> (1 : 1) <sup>d</sup>	415 (5.27) 525 (5.25)	583 (3.73); 615 (3.55); 663 (3.75); 723 (4.19); 844 (3.26); 962 (3.26)

<sup>a</sup> 1 : 1 Physical mixture of compound **5** & **6**. <sup>b</sup> 1 : 1 Physical mixture of compound **5** & **7**. <sup>c</sup> 1 : 1 Physical mixture of compound **5** & **8**. <sup>d</sup> 1 : 1 Physical mixture of compound **5** & **9**. Concentration of solution used for Soret band is  $1 \times 10^{-6}$  M and for Q-band is  $1 \times 10^{-5}$  M.

**Table 3** Redox potential and emission data of dyads **1–4** along with their corresponding monomers

Compound	Oxidation <sup>a</sup> (V)				Reduction <sup>a</sup> (V)				$\Phi_{515}^b$ (%Q)	$\Phi_{550}^b$ (%Q)
<b>1</b>	—	1.00	1.24	1.43	−1.07	−1.38	−1.50	—	0.016 (0)	0.065 (32)
<b>2</b>	—	1.00	1.24	1.51	−0.96	−1.24	−1.51	—	0.0076 (4)	0.058 (39)
<b>3</b>	0.70	1.00	1.23	—	−0.90	−1.11	−1.52	−1.68	—	0.037 (60)
<b>4</b>	0.61	1.04	1.24	—	−0.80	−1.02	−1.51	−1.68	—	0.016 (83)
<b>5</b>	—	1.01	1.24	—	—	−1.17	−1.52	—	—	0.095
<b>6</b>	—	1.02	—	1.43	−1.09	—	−1.41	—	0.016	—
<b>7</b>	—	—	1.18	1.52	−0.96	−1.24	—	—	0.0079	—
<b>8</b>	0.68	—	1.22	—	−0.94	−1.18	—	−1.63	—	—
<b>9</b>	0.58	1.05	1.15	—	−0.80	−1.03	—	−1.66	—	—

<sup>a</sup> Redox data recorded in dichloromethane containing 0.1 M TBAP as supporting electrolyte at 50 mV s<sup>−1</sup> scan rate. <sup>b</sup> (%Q) Denotes percentage of quenching of fluorescence quantum yield in dichloromethane solvent.

reduction at −1.24 V were due to both components. Similarly, all other dyads **1**, **3** and **4** also showed features of both the constituent components with almost no change in their redox potentials compared to their corresponding independent monomers. Thus, the electrochemical studies indicate that both components in the dyads retain most of their independent features in dyads.

In order to understand the singlet excited state properties of dyads **1–4**, preliminary studies of the steady state fluorescence properties of dyads **1–4** were carried out. The steady state fluorescence spectra of dyads **1** and **2** along with their 1 : 1 mixture of corresponding monomers are shown in Fig. 4 and the relevant data are tabulated in Table 3. In dyads **1** and **2**, the basal Al(III) porphyrin and axial N<sub>3</sub>S and N<sub>2</sub>S<sub>2</sub> porphyrins are fluorescent but in dyads **3** and **4**, the axial thiasapphyrin and thiarubyrin are non-fluorescent. Hence the steady state fluorescence experiments were carried out at 550 nm where Al(III) porphyrin absorbs relatively strongly compared to axial macrocycles, and also at 515 nm for dyads **1** and **2** where the

axial N<sub>3</sub>S and N<sub>2</sub>S<sub>2</sub> porphyrin units, respectively, absorb strongly compared to Al(III) porphyrin. Thus, on excitation of dyads **1** and **2** at 515 nm, the emission was mainly observed from axial N<sub>3</sub>S and N<sub>2</sub>S<sub>2</sub> porphyrin units, respectively, and the quantum yields were almost in the same range as their respective monomeric porphyrins. However, for dyads **1** and **2**, on excitation at 550 nm where Al(III) porphyrin absorbs relatively strongly, the major emission was noted mainly from the Al(III) porphyrin unit along with a minor emission from the axial thiaporphyrin porphyrin unit (Fig. 4). Under the same excitation conditions, their corresponding 1 : 1 mixture of monomers showed emission exclusively from the Al(III) porphyrin unit and absolutely no emission was noted from the axial thiaporphyrin units. The excitation spectra of dyads **1** and **2**, recorded at 700 nm where the emission was exclusively due to axial N<sub>3</sub>S and N<sub>2</sub>S<sub>2</sub> porphyrin units, showed absorption bands due to Al(III) porphyrin as well as axial N<sub>3</sub>S or N<sub>2</sub>S<sub>2</sub> porphyrin units. Furthermore, the quantum yield of Al(III) porphyrin unit in dyads **1** and **2** was reduced by 30–40% as

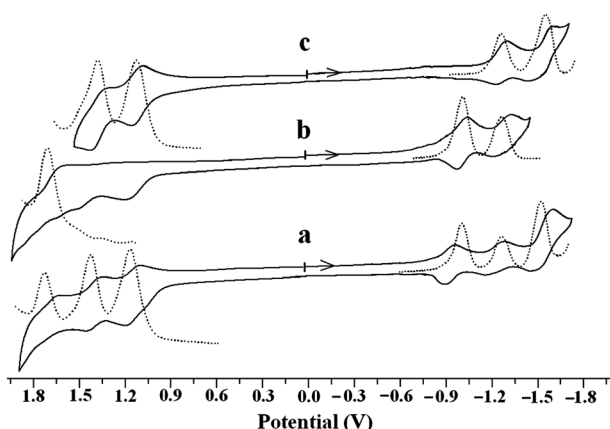


**Fig. 3** Comparison of redox waves and differential pulse voltammetry (dotted line) of (a) dyad **2** along with its constituent monomers (b) **7** and (c) **5** recorded in dichloromethane using 0.1 M tetrabutylammonium perchlorate (TBAP) as the supporting electrolyte and saturated calomel electrode (SCE) as the reference electrode at 50 mV s<sup>-1</sup> scan rate.

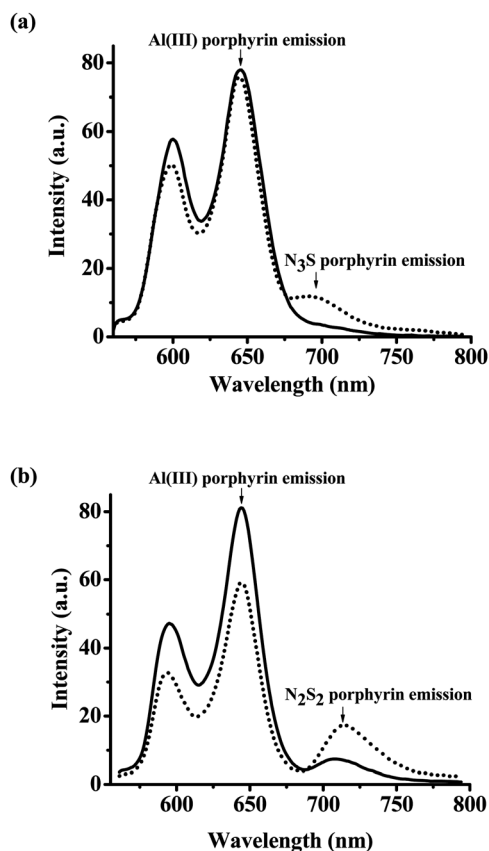


**Fig. 4** Fluorescence spectra of (a) dyad **1** (dotted line) along with a 1 : 1 mixture (solid line) of the corresponding constituent monomers **5** and **6** and (b) dyad **2** (dotted line) along with a 1 : 1 mixture (solid line) of the corresponding constituent monomers **5** and **7** recorded in dichloromethane by exciting at wavelength of 550 nm.

compared to monomeric Al(III) porphyrin. These results indicate that there is a possibility of energy transfer from the basal Al(III) porphyrin to the axial N<sub>3</sub>S porphyrin unit in dyad **1** and the N<sub>2</sub>S<sub>2</sub> porphyrin unit in dyad **2**. Besides energy

transfer, which is mainly responsible for quenching the fluorescence of the Al(III) porphyrin subunit in dyads, we cannot rule out the possibility of photoinduced electron transfer (PET) from the ground state of the axial thiaporphyrin subunit (N<sub>3</sub>S and N<sub>2</sub>S<sub>2</sub> porphyrins) to the singlet state of Al(III) porphyrin dyads **1** and **2**. Hence we evaluated the relationship of the energy levels in dyads **1** and **2** with eqn (1) and (2), respectively, using fluorescence and redox potential data.

$$\Delta G(^1\text{AIP} \rightarrow \text{N}_3\text{S}) = E_{\text{CT}}(\text{AIP}^+ \text{N}_3\text{S}^-) - E_{0-0}(\text{AIP}) \quad (1)$$

$$\Delta G(^1\text{AIP} \rightarrow \text{N}_2\text{S}_2) = E_{\text{CT}}(\text{AIP}^+ \text{N}_2\text{S}_2^-) - E_{0-0}(\text{AIP}) \quad (2)$$

The singlet excited and the charge transfer states for dyads **1** and **2** are shown in Fig. 5. As is clear from Fig. 5, in both these dyads the excited singlet state of the donor Al(III) porphyrin is higher than the charge transfer state as well as the singlet state of the acceptor thiaporphyrin unit. Thus, the free energy change  $\Delta G_{\text{PET}}$  is negative for dyads **1** and **2**, indicating that electron transfer is also possible in addition to energy transfer in these two dyads. The quenching of the fluorescence intensity of the basal Al(III) porphyrin in dyads **1** and **2** can be rationalized in terms of both the intramolecular energy transfer and the photoinduced electron transfer between the components in dyads **1** and **2**. For dyads **3** and **4**, on excitation at 550 nm, the emission was noted only from the Al(III) porphyrin unit since the axial sapphyrin unit in dyad **3** and rubyrin unit in dyad **4** are non-fluorescent chromophores (S17–S18, ESI<sup>†</sup>). However, the quantum yield of the Al(III) porphyrin unit in dyads **3** and **4** are reduced by 60–80% compared to the monomeric Al(III) porphyrin, which may be attributed to the presence of the low lying singlet state energy levels of axial expanded heteroporphyrin units, which significantly quench the fluorescence of the basal Al(III) porphyrin. More detailed studies are under investigation.

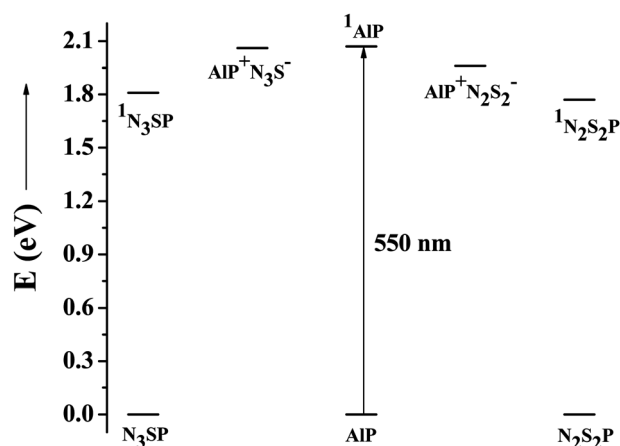


**Fig. 5** A generalized energy level diagram illustrating the singlet and charge transfer states for dyads **1** and **2**.

## Quantum chemical studies

The minimum energy structures of four dyads **1–4** calculated at B3LYP/6-31G(d) level of theory are displayed in Fig. 6. This choice of DFT functional and basis set should be sufficient for these metalloporphyrin based multiporphyrin dyads. It is observed from fully optimized structures of four dyads **1–4** that the basal Al(III) porphyrin unit is not planar in any of these four dyads **1–4** (S19, ESI†). The Al(III) ion of the basal scaffold is pulled upward towards the corresponding axial chromophore from the mean plane of four pyrrole nitrogens of the Al(III) porphyrin unit in all four dyads. The out-of-plane displacement of the Al(III) ion is about 12° from

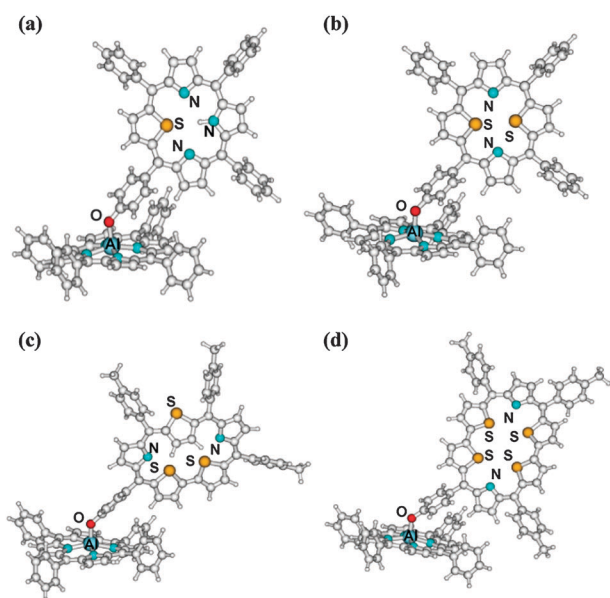


**Fig. 6** Fully optimized structures of (a) dyad **1**, (b) dyad **2**, (c) dyad **3** and (d) dyad **4** applying B3LYP/6-31G(d) level of theory.

the mean plane of the four pyrrole nitrogens in dyads **1–4**. The four Al–N bond lengths are nonequivalent for individual dyads **1–4**. But in the dyads **1–4**, the average Al–N bond length is 2.03 Å, which is in the same range as that found in crystallographic data for Al(III) porphyrins based other derivatives.<sup>4n,6h–1,7b–c</sup> The dihedral angles (avg. 68°–70°) between the *meso*-phenyl rings and the mean-porphyrin-plane of basal Al(III) porphyrin units are almost in the same range in all the cases. On the other hand, the axial N<sub>3</sub>S and N<sub>2</sub>S<sub>2</sub> units are almost planar in dyads **1** and **2**, respectively, whereas the axial sapphyrin unit in dyad **3**, and the axial rubyrin unit in dyad **4** are nonplanar (S19, ESI†). In dyad **3**, one of the thiophene rings is inverted and distorted from the mean plane of the sapphyrin unit, which is commonly observed for sapphyrin macrocycles.<sup>11</sup> In dyad **4**, because of the large ring size, the axial rubyrin unit is also twisted. Frontier molecular orbitals (FMOs) calculations suggest that in the case of dyads **1–3**, axial units and the basal Al(III) porphyrin unit mainly participate in the highest molecular orbital (HOMO) and the lowest molecular orbital (LUMO), respectively (S20, ESI†). In the case of dyad **4**, only the axial rubyrin unit is involved in both the HOMO and LUMO orbitals (S20, ESI†). It is to be noted that neither the bridging oxygen atom nor the central metal Al(III) ion participates in either of the FMOs (HOMO and LUMO).

Vertical electronic transitions are calculated for these four dyads **1–4** applying the B3LYP functional under TD-DFT formalism with the ground state (*S*<sub>0</sub>) optimized structures predicted at the B3LYP level of theory. The COSMO model is also applied to account for the macroscopic solvent effect in dichloromethane solvent. Results on a few low lying electronic transitions originating from the basal Al(III) porphyrin unit in the Soret band region are presented in Table 4, showing the major electronic transitions involved in the observed Soret bands of these systems. As it is shown in Table 4, the strong electronic transitions having oscillator strength *f* ≥ 1.1 are initiated mainly from the HOMO – 2 and HOMO – 3 orbitals in all four cases. But in the case of dyads **3** and **4**, the strongest

**Table 4** Electronic transitions, oscillator strengths (*f*), transition wavelengths (λ, nm), and coefficients of wave function obtained in the Soret band region (originated from basal Al(III) porphyrin unit) calculated based on TD-DFT (B3LYP) method employing 6-31G(d) basis set in the dyads **1–4**

Compounds	Assignment of electronic transitions <sup>a</sup>	Oscillator strength ( <i>f</i> )	Transition wave length (nm)	Coefficient of wave function <sup>b</sup>
<b>1</b>	HOMO – 4 → LUMO	1.11	380	0.21
	HOMO – 2 → LUMO			0.36
	HOMO – 3 → LUMO			0.17
	HOMO – 7 → LUMO + 2			0.26
<b>2</b>	HOMO – 5 → LUMO + 2	1.44	377	0.29
	HOMO – 3 → LUMO + 1			0.29
	HOMO – 2 → LUMO			0.22
	HOMO – 1 → LUMO + 3			0.25
<b>3</b>	HOMO – 4 → LUMO	1.09	380	0.18
	HOMO – 4 → LUMO + 1			0.43
	HOMO – 3 → LUMO			0.27
	HOMO – 2 → LUMO			0.30
<b>4</b>	HOMO – 4 → LUMO + 1	1.16	380	0.39
	HOMO – 3 → LUMO + 1			0.30
	HOMO – 3 → LUMO + 2			0.27
	HOMO – 2 → LUMO + 2			0.35

<sup>a</sup> Only the excited states with oscillator strengths *f* > 1.0 are shown (from the calculated forty low-lying excited states). <sup>b</sup> Only the electronic transitions with coefficients of wave function above 0.15 are shown.



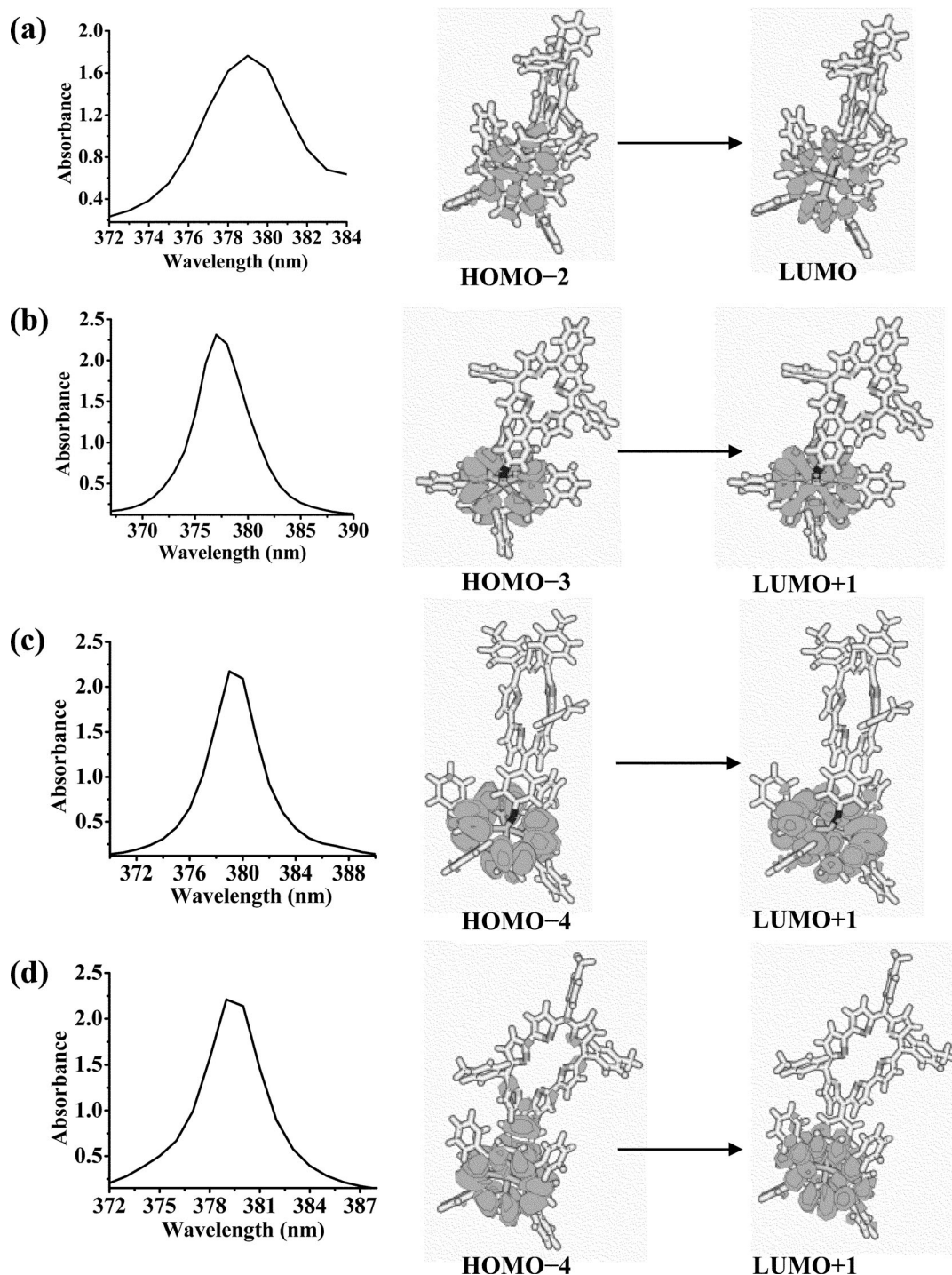


**Fig. 7** Simulated UV-vis spectra of (a) dyad 1, (b) dyad 2, (c) dyad 3 and (d) dyad 4 in the Soret band region. Simulation of these absorption profiles was carried out from forty low lying vertical excited states with Gaussian line shape.

electronic transitions are initiated from the HOMO – 4 orbital. The major electronic transitions occur to either the LUMO or LUMO + 1 orbital in all these systems. In both these molecular orbitals, mainly macrocyclic ring  $\pi^*$  electrons participate with a small contribution from the *meso* substituents. UV-vis spectra of these four dyads (1–4) in the Soret band region are simulated following a Gaussian line shape and the spectra are depicted in Fig. 7. The calculated absorption maxima ( $\lambda_{\text{max}}$ ) are about 40 nm

blue shifted in comparison to the present experimental values. Due to the large size of these dyad systems, excited state calculations at a higher level of theory with large basis functions are beyond the scope at present. However, these calculations are able to assign the electronic transitions involved in these dyad systems showing the origin of the Soret band. The excited state calculations do depict that the Soret bands in all these four dyads are in the same wavelength region.

## Conclusions

We described the synthesis of four novel Al(III) porphyrin based axial-bonding type dyads containing thiaporphyrins or expanded thiaporphyrins as axial ligands for the first time. The dyads were prepared in high yields and are stable for column chromatographic purification conditions and soluble in common organic solvents. 1D and 2D NMR studies helped in deducing the structures of dyads. All our efforts to obtain single crystals of these dyads failed. The geometry of these multiporphyrin dyads was calculated at the B3LYP/6-31G(d) level of theory. The absorption and electrochemical studies of dyads showed the features of both the components, supporting that the two macrocycles retain their individual properties in dyads. Excited state calculations are carried out at the TD-DFT level of theory with the B3LYP functional and the origin of Soret band in these dyads is assigned to different electronic transitions. The steady state fluorescence studies showed the possibility of singlet-singlet energy transfer from the Al(III) porphyrin to the axial thiaporphyrin unit in dyads **1** and **2**. Currently, we are exploring the possibility of the synthesis of Al(III) porphyrin based axial bonding type arrays containing other macrocycles, such as corroles/core-modified corroles, as axial units.

## Experimental section

All general chemicals and solvents were procured from S D. Fine Chemicals, India. Column chromatography was performed by using basic alumina obtained from Sisco Research Laboratories, India. Tetrabutylammonium perchlorate was purchased from Fluka and used without further purification.

<sup>1</sup>H NMR spectra were recorded with Varian and Bruker 400 MHz instrument using tetramethylsilane as an internal standard. <sup>1</sup>H-<sup>1</sup>H COSY experiments were performed on a Bruker 400 MHz instrument. All NMR measurements were carried out at room temperature in deuterated chloroform. Absorption and steady state fluorescence spectra, respectively, were obtained with a Perkin-Elmer Lambda-35 and Varian Cary Eclipse fluorescence spectrophotometer, respectively. The fluorescence quantum yields ( $\Phi_f$ ) of Al(III) porphyrin in dyads **1-4** were estimated from the emission and absorption spectra by the comparative method<sup>13</sup> using ZnTPP as a standard ( $\Phi_f = 0.033$ ). MALDI-TOF spectra were obtained from Axima-CFR manufactured by Kratos Analyticals. Cyclic Voltammetric (CV) and Differential Pulse Voltammetric (DPV) studies were carried out with a BAS electrochemical system utilizing the three electrode configuration consisting of a glassy carbon (working electrode), platinum wire (auxiliary electrode), and saturated calomel (reference electrode) electrodes in dry dichloromethane using 0.1 M tetrabutylammonium perchlorate (TBAP) as the supporting electrolyte.

## Theoretical methods

DFT calculations were carried out on four dyad systems (**1-4**) to find out the minimum energy structures and to study their electronic properties. Searches for these structures were performed in the ground electronic state ( $S_0$ ) applying Becke's three parameters correlated hybrid density functional, B3LYP

adopting 6-31G(d) atomic basis functions, which include at least 3200 primitive Gaussian functions in total. Equilibrium structures of these systems were calculated based on full geometry optimization following a Newton Raphson procedure. Excited state calculations were carried out by applying a TD-DFT procedure with the B3LYP functional for forty low lying vertical electronic transitions on  $S_0$  state optimized structures using the COSMO solvation model to account for the solvent ( $\text{CH}_2\text{Cl}_2$ ) effect with the same set of basis functions. Simulation of absorption profiles was carried out from 40 low lying excited states with a Gaussian line shape, *i.e.*

$$\varepsilon(E) = A \sum_i \frac{f_i}{\Delta_i} \exp\left(-B \frac{(E - E_i)^2}{\Delta_i^2}\right),$$

where,  $\varepsilon$ ,  $E$ ,  $f$ ,  $\Delta$  are molar extinction coefficient, transition energy, oscillator strength and half band-width, respectively. UV-vis spectra were generated by considering the full-width at half-maximum (fwhm) as 100 nm. The total integrated intensity under the absorption profile was kept equal to the sum of all the oscillator strengths. All the electronic structure calculations were carried out by applying the GAMESS suite of *ab initio* programs.<sup>14</sup> Visualization of molecular structures and orbital contour plots were carried out using molden visualization software.<sup>15</sup>

## Syntheses

The precursor porphyrins, *viz.* 5,10,15,20-tetraphenylporphyrin ( $\text{H}_2\text{TPP}$ ), 5-(4-hydroxyphenyl)-10,15,20-tri(p-tolyl)-21-thiaporphyrin<sup>12a</sup> (**6**), 5-(4-hydroxyphenyl)-10,15,20-tri(p-tolyl)-21,23-dithiaporphyrin<sup>12a</sup> (**7**), 5-(4-hydroxyphenyl)-10,15,20-tritoyl-25,27,29-trithiasapphyrin<sup>12b</sup> (**8**) and 5-(4-hydroxyphenyl)-10,19,24-tritoyl-29,30,32,33-tetrathiarubyrin<sup>12b</sup> (**9**) were synthesized by following the established methods. Al(III) porphyrin derivatives [(TPP)Al<sup>III</sup>Cl] and [(TPP)Al<sup>III</sup>OH]<sup>9</sup> (**5**) were synthesized and purified according to the literature reported procedures.

### General synthesis of axial bonding type Al(III) porphyrin based dyads (**1-4**)

The dyads **1-4** were synthesised by refluxing one equivalent of [(TPP)Al<sup>III</sup>OH] (**5**) and 1.2 equivalents of corresponding monohydroxy-thiaporphyrin/expandedthiaporphyrin (**6-9**), respectively, in dry benzene (30 mL) for 12 h under a nitrogen atmosphere. The solvent was evaporated under reduced pressure and the resulting crude product was subjected to neutral alumina column chromatography. The trace amount of unreacted [(TPP)Al<sup>III</sup>OH] was removed as the first purple coloured band with  $\text{CH}_2\text{Cl}_2$  and the corresponding desired product was then collected with a  $\text{CH}_2\text{Cl}_2$ /acetone (0.5-1%) mixture of solvents. The solvent was removed under reduced pressure and the product was recrystallized from a  $\text{CH}_2\text{Cl}_2$ /*n*-hexane mixture to afford pure dyads **1-4** in decent yields.

**Dyad 1.** 70% Yield; Mp > 300 °C; <sup>1</sup>H NMR (400 MHz,  $\text{CDCl}_3$ ):  $\delta$  -2.79 (s, 2H, inner NH), 2.88 (d,  $J = 8.3$  Hz, 2H, bridging phenyl), 6.74 (d,  $J = 8.4$  Hz, 2H, bridging phenyl), 7.68-7.80 (m, 20H, Ar), 8.11-8.26 (m, 16H, [ $\beta$ -pyrrole + Ar]), 8.36 (d,  $J = 4.5$  Hz, 1H,  $\beta$ -pyrrole), 8.55 (d,  $J = 4.5$  Hz, 1H,  $\beta$ -pyrrole), 8.65 (d,  $J = 4.6$  Hz, 1H,  $\beta$ -pyrrole), 8.85 (s, 2H,

$\beta$ -thiophene), 9.16 (s, 8H,  $\beta$ -pyrrole Al[III]-porphyrin), 9.18 (d,  $J = 5.2$  Hz, 1H,  $\beta$ -thiophene), 9.47 (d,  $J = 5.2$  Hz, 1H,  $\beta$ -thiophene) ppm. MALDI-TOF:  $m/z$  (%) = 1286.4  $[M]^+$ . Elemental analysis: Calcd (%) for  $C_{88}H_{57}AlN_7OS$ : C 82.09, H 4.46, N 7.61, S 2.49; Found: C 82.10, H 4.43, N 7.63, S 2.51.

**Dyad 2.** 80% Yield; Mp > 300 °C;  $^1H$  NMR (400 MHz,  $CDCl_3$ ):  $\delta$  2.89 (d,  $J = 8.4$  Hz, 2H, bridging phenyl), 6.73 (d,  $J = 8.3$  Hz, 2H, bridging phenyl), 7.70–7.83 (m, 20H, Ar), 8.09 (d,  $J = 4.5$  Hz, 1H,  $\beta$ -pyrrole), 8.17–8.25 (m, 15H, Ar), 8.43 (d,  $J = 4.5$  Hz, 1H,  $\beta$ -pyrrole), 8.63 (br s, 2H,  $\beta$ -pyrrole), 9.09 (d,  $J = 5.1$  Hz, 1H,  $\beta$ -thiophene), 9.17 (m, 8H,  $\beta$ -pyrrole Al[III]-porphyrin), 9.41 (d,  $J = 5.1$  Hz, 1H,  $\beta$ -thiophene), 9.60 (s, 2H,  $\beta$ -thiophene) ppm. MALDI-TOF:  $m/z$  (%) = 1301.9  $[M-1]^+$ . Elemental analysis: Calcd (%) for  $C_{88}H_{56}AlN_6OS_2$ : C 81.02, H 4.33, N 6.44, S 4.91; Found: C 81.05, H 4.39, N 6.42, S 4.92.

**Dyad 3.** 65% Yield; Mp > 300 °C;  $^1H$  NMR (400 MHz,  $CDCl_3$ ):  $\delta$  -0.69 (d,  $J = 5.4$  Hz, 1H,  $\beta$ -thiophene), -0.61 (d,  $J = 5.4$  Hz, 1H,  $\beta$ -thiophene), 2.60–2.72 (m, 6H,  $CH_3$ ), 2.82 (s, 3H,  $CH_3$ ), 2.91 (d,  $J = 7.9$  Hz, 2H, bridging phenyl), 6.80 (d,  $J = 8.2$  Hz, 2H, bridging phenyl), 7.54–7.80 (m, 18H, Ar), 8.05 (d,  $J = 4.4$  Hz, 1H,  $\beta$ -pyrrole), 8.14–8.29 (m, 15 H,  $\beta$ -pyrrole + Ar), 8.47 (d,  $J = 4.4$  Hz, 1H,  $\beta$ -pyrrole), 8.59 (d,  $J = 4.4$  Hz, 1H,  $\beta$ -pyrrole), 9.12 (d,  $J = 4.6$  Hz, 1H,  $\beta$ -thiophene), 9.18 (s, 8H,  $\beta$ -pyrrole Al[III]-porphyrin), 9.68 (d,  $J = 4.6$  Hz, 1H,  $\beta$ -thiophene), 9.90 (d,  $J = 4.5$  Hz, 1H,  $\beta$ -thiophene), 10.05 (d,  $J = 4.6$  Hz, 1H,  $\beta$ -thiophene) ppm. MALDI-TOF:  $m/z$  (%) = 1427.3  $[M]^+$ , 1425.9  $[M-1]^+$ . Elemental analysis: Calcd (%) for  $C_{95}H_{63}AlN_6OS_3$ : C 79.92, H 4.45, N 5.89, S 6.74; Found: C 79.97, H 4.43, N 5.90, S 6.73.

**Dyad 4.** 73% Yield; Mp > 300 °C;  $^1H$  NMR (400 MHz,  $CDCl_3$ ):  $\delta$  2.78 (s, 3H,  $CH_3$ ), 2.84 (s, 3H,  $CH_3$ ), 2.89 (s, 3H,  $CH_3$ ), 3.06 (d,  $J = 8.3$  Hz, 2H, bridging phenyl), 7.04 (d,  $J = 8.3$  Hz, 2H, bridging phenyl), 7.75–7.82 (m, 18H, Ar), 8.31–8.44 (m, 15H, [ $\beta$ -pyrrole + Ar]), 8.77 (d,  $J = 4.5$  Hz, 1H,  $\beta$ -pyrrole), 9.01–9.04 (m, 2H,  $\beta$ -pyrrole), 9.27 (s, 8H,  $\beta$ -pyrrole Al[III]-porphyrin), 9.76 (d,  $J = 5.0$  Hz, 1H,  $\beta$ -thiophene), 10.39–10.44 (m, 3H,  $\beta$ -thiophene), 11.24 (d,  $J = 5.1$  Hz, 1H,  $\beta$ -thiophene), 11.47 (d,  $J = 5.0$  Hz, 1H,  $\beta$ -thiophene), 11.50–11.53 (superimposed dd, 2H,  $\beta$ -thiophene) ppm. MALDI-TOF:  $m/z$  (%) = 1509.4  $[M]^+$ . Elemental analysis: Calcd (%) for  $C_{99}H_{68}AlN_6OS_4$ : C 78.59, H 4.53, N 5.55, S 8.48; Found: C 78.60, H 4.55, N 5.53, S 8.46.

## Acknowledgements

MR thanks BRNS, India for funding the project and AG thanks CSIR for fellowship. Computer Centre, BARC is gratefully acknowledged for generous CPU time in ANUPAM parallel computer systems.

## References

- (a) J. K. M. Sanders, in *The Porphyrin Handbook*, ed. K. M. Kadish, K. M. Smith and R. Guilard, Academic Press, New York, 2000, vol. 3, pp. 347–368; (b) J. K. M. Sanders, N. Bampos, Z. Clyde-Watson, S. L. Darling, J. C. Hawley, H.-J. Kim, C. C. Mak and S. J. Webb, in *The Porphyrin Handbook*,

- ed. K. M. Kadish, K. M. Smith and R. Guilard, Academic Press, New York, 2000, vol. 3, p. 148; (c) D. Gust and T. A. Moore, in *The Porphyrin Handbook*, ed. K. M. Kadish, K. M. Smith and R. Guilard, Academic Press, London, 2000, vol. 8, pp. 153–167; (d) D. Holten, D. F. Bocian and J. S. Lindsey, *Acc. Chem. Res.*, 2002, **35**, 57; (e) G. Simonneaux and P. L. Maux, *Coord. Chem. Rev.*, 2002, **228**, 43; (f) M. Ayabe, A. Ikeda, Y. Kubo, M. Takeuchi and S. Shinkai, *Angew. Chem., Int. Ed.*, 2002, **41**, 2790; (g) M. L. Merlau, M. P. Mejia, S. B. T. Nguyen and J. T. Hupp, *Angew. Chem., Int. Ed.*, 2001, **40**, 4239; (h) K. Sugou, K. Sasaki, T. Iwaki and Y. Kuroda, *J. Am. Chem. Soc.*, 2002, **124**, 1182; (i) E. Iengo, E. Zangrando, R. Minatel and E. Alessio, *J. Am. Chem. Soc.*, 2002, **124**, 1003.
- (a) K. S. Suslick, N. A. Rakow, M. E. Kosal and J.-H. Chou, *J. Porphyrins Phthalocyanines*, 2000, **4**, 407; (b) A. K. Burrell, D. L. Officer, P. G. Plieger and D. C. W. Reid, *Chem. Rev.*, 2001, **101**, 2751; (c) H. Shinokubo and A. Osuka, *Chem. Commun.*, 2009, 1011; (d) D. H. Yoon, S. B. Lee, K.-H. Yoo, J. Kim, J. K. Lim, N. Aratani, A. Tsuda, A. Osuka and D. Kim, *J. Am. Chem. Soc.*, 2003, **125**, 11062; (e) W. J. Cho, Y. Cho, S. K. Min, W. Y. Kim and K. S. Kim, *J. Am. Chem. Soc.*, 2011, **133**, 9364; (f) J. Otsuki, E. Nagamine, T. Kondo, K. Iwasaki, M. Asakawa and K. Miyake, *J. Am. Chem. Soc.*, 2005, **127**, 10400; (g) N. Aratani, D. Kim and A. Osuka, *Acc. Chem. Res.*, 2009, **42**, 1922; (h) J. A. Hutchison, P. J. Santic, P. R. Brotherhood, C. Scholes, I. M. Blake, K. P. Ghiggino and M. J. Crossley, *J. Phys. Chem. C*, 2009, **113**, 11796; (i) J. Yang, M. Park, Z. S. Yoon, T. Hori, X. Peng, N. Aratani, P. Dedeker, J.-i. Hotta, H. Uji-i, M. Sliwa, J. Hofkens, A. Osuka and D. Kim, *J. Am. Chem. Soc.*, 2008, **130**, 1879; (j) M.-C. Yoon, S. Cho, P. Kim, T. Hori, N. Aratani, A. Osuka and D. Kim, *J. Phys. Chem. B*, 2009, **113**, 15074; (k) D. C. G. Gotz, T. Bruhn, M. O. Senge and G. Bringmann, *J. Org. Chem.*, 2009, **74**, 8005; (l) S. Cho, M.-C. Yoon, K. S. Kim, P. Kim and D. Kim, *Phys. Chem. Phys.*, 2011, **13**, 16175; (m) A. Ryan, A. Gehrold, R. Perusitti, M. Pintea, M. Fazekas, O. B. Locos, F. Blaikie and M. O. Senge, *Eur. J. Org. Chem.*, 2011, 5817; (n) T. Ikeda, N. Aratani and A. Osuka, *Chem.-Asian J.*, 2009, **4**, 1248; (o) C.-A. Wu, C.-L. Chiu, C.-L. Mai, Y.-S. Lin and C.-Y. Yeh, *Chem.-Eur. J.*, 2009, **15**, 4534.
- (a) T. Imamura and K. Fukushima, *Coord. Chem. Rev.*, 2000, **198**, 133; (b) J. Wojaczynski and L. Latos Grazynski, *Coord. Chem. Rev.*, 2000, **204**, 113; (c) S. George and I. Goldberg, *Cryst. Growth Des.*, 2006, **6**, 755; (d) X. Peng, Y. Huang, C. Gao, J. Peng, N. Komatsu, A. Osuka and Y. Cao, *J. Phys. Chem. C*, 2010, **114**, 18449; (e) J. Yu, S. Mathew, B. S. Flavel, M. R. Johnston and J. G. Shapter, *J. Am. Chem. Soc.*, 2008, **130**, 8788; (f) K. Chichak and N. R. Branda, *Chem. Commun.*, 2000, 1211; (g) A. D'Urso, M. E. Fragalà and R. Purrello, *Chem. Commun.*, 2012, **48**, 8165; (h) F. Atefi, J. C. Mc. M. and D. P. Arnold, *Dalton Trans.*, 2007, 2163; (i) C. M. Drain, F. Nifatis, A. Vasenko and J. D. Batteas, *Angew. Chem., Int. Ed.*, 1998, **37**, 2344; (j) K.-ya Tomizaki, L. Yu, L. Wei, D. F. Bocian and J. S. Lindsey, *J. Org. Chem.*, 2003, **68**, 8199; (k) Y. Nakamura, N. Aratani and A. Osuka, *Chem. Soc. Rev.*, 2007, **36**, 831.
- (a) P. P. Kumar, G. Premaladha and B. G. Maiya, *Chem. Commun.*, 2005, 3823; (b) P. P. Kiran, D. R. Reddy, B. G. Maiya, A. K. Dharmadhikari, G. R. Kumar and D. N. Rao, *Opt. Commun.*, 2005, **252**, 150; (c) D. R. Reddy and B. G. Maiya, *J. Phys. Chem. A*, 2003, **107**, 6326; (d) D. R. Reddy and B. G. Maiya, *J. Porphyrins Phthalocyanines*, 2002, **6**, 3; (e) A. A. Kumar, L. Giribabu, D. R. Reddy and B. G. Maiya, *Inorg. Chem.*, 2001, **40**, 6757; (f) D. R. Reddy and B. G. Maiya, *Chem. Commun.*, 2001, 117; (g) L. Giribabu, T. A. Rao and B. G. Maiya, *Inorg. Chem.*, 1999, **38**, 4971; (h) T. A. Rao and B. G. Maiya, *Inorg. Chem.*, 1996, **35**, 4829; (i) T. A. Rao and B. G. Maiya, *J. Chem. Soc., Chem. Commun.*, 1995, (9), 939; (j) B. G. Maiya, N. Bampos, A. A. Kumar, N. Feeder and J. K. M. Sanders, *New J. Chem.*, 2001, **25**, 797; (k) J. C. Hawley, N. B. Bampos, R. J. Abraham and J. K. M. Sanders, *Chem. Commun.*, 1998, 661; (l) H.-J. Kim, N. Bampos and J. K. M. Sanders, *J. Am. Chem. Soc.*, 1999, **121**, 8120; (m) S. J. Webb and J. K. M. Sanders, *Inorg. Chem.*, 2000, **39**, 5920; (n) G. J. E. Davidson, L. A. Lane, P. R. Raithby, J. E. Warren, C. V. Robinson and J. K. M. Sanders, *Inorg. Chem.*, 2008, **47**, 8721.
- (a) G. D. Fallon, M. A.-P. Lee, S. J. Langford and P. J. Nichols, *Org. Lett.*, 2002, **4**, 1895; (b) S. J. Langford, M. J. Latter and



- J. Beckmann, *Inorg. Chem. Commun.*, 2005, **8**, 920; (c) S. J. Langford and C. P. Woodward, *CrystEngComm*, 2007, **9**, 218; (d) H.-J. Kim, H. J. Jo, J. Kim, S.-Y. Kim, D. Kim and K. Kim, *CrystEngComm*, 2005, **7**, 417; (e) H. J. Jo, S. H. Jung and H.-J. Kim, *Bull. Korean Chem. Soc.*, 2004, **25**, 1869; (f) U. Michelsen and C. A. Hunter, *Angew. Chem., Int. Ed.*, 2000, **39**, 764; (g) R. A. Haycock, C. A. Hunter, D. A. James, U. Michelsen and L. R. Sutton, *Org. Lett.*, 2000, **2**, 2435; (h) A. Tsuda, T. Nakamura, S. Sakamoto, K. Yamaguchi and A. Osuka, *Angew. Chem., Int. Ed.*, 2002, **41**, 2817; (i) L. J. Twyman and A. S. H. King, *Chem. Commun.*, 2002, 910; (j) D. Furutsu, A. Satake and Y. Kobuke, *Inorg. Chem.*, 2005, **44**, 4460; (k) R. Takahashi and Y. Kobuke, *J. Org. Chem.*, 2005, **70**, 2745; (l) T. Xu, R. Lu, X. Liu, X. Zheng, X. Qiu and Y. Zhao, *Org. Lett.*, 2007, **9**, 797; (m) T. Lazarides, S. Kuhri, G. Charalambidis, M. K. Panda, D. M. Guldi and A. G. Coutsolelos, *Inorg. Chem.*, 2012, **51**, 4193.
- 6 (a) H. Sugimoto, T. Kimura and S. Inoue, *J. Am. Chem. Soc.*, 1999, **121**, 2325; (b) K. Konishi, T. Aida and S. Inoue, *J. Org. Chem.*, 1990, **55**, 816; (c) Y. Hirai, T. Aida and S. Inoue, *J. Am. Chem. Soc.*, 1989, **111**, 3062; (d) T. Arai and S. Inoue, *Tetrahedron*, 1990, **46**, 149; (e) T. Yasuda, T. Aida and S. Inoue, *Bull. Chem. Soc. Jpn.*, 1985, **58**, 3931; (f) T. Arai, H. Murayama and S. Inoue, *J. Org. Chem.*, 1989, **54**, 414; (g) P. K. Poddutoori, A. S. D. Sandanayaka, T. Hasobe, O. Ito and A. Est, *J. Phys. Chem. B*, 2010, **114**, 14348; (h) R. Guilard, A. Zrineh, A. Tabard, A. Endo, B. C. Han, C. Lecomte, M. Souhassou, A. Habbou, M. Ferhat and K. M. Kadish, *Inorg. Chem.*, 1990, **29**, 4476; (i) S. Richeter, J. Thion, A. Lee and D. Leclercq, *Inorg. Chem.*, 2006, **45**, 10049; (j) P. K. Poddutoori, P. Poddutoori, B. G. Maiya, T. K. Prasad, Y. E. Kandrashkin, S. Vasil'ev, D. Bruce and A. Est, *Inorg. Chem.*, 2008, **47**, 7512; (k) S. Inoue and N. Takeda, *Bull. Chem. Soc. Jpn.*, 1977, **50**, 984; (l) A. Harriman, *J. Chem. Soc., Faraday Trans. 1*, 1982, **78**, 2727; (m) Y. Kaizu, H. Maekawa and H. Kobayashi, *J. Phys. Chem.*, 1986, **90**, 4234.
- 7 (a) P. P. Kumar and B. G. Maiya, *New J. Chem.*, 2003, **27**, 619; (b) G. J. E. Davidson, L. H. Tong, P. R. Raithby and J. K. M. Sanders, *Chem. Commun.*, 2006, 3087; (c) G. A. Metselaar, J. K. M. Sanders and J. de Mendoza, *Dalton Trans.*, 2008, 588; (d) E. Iengo, G. D. Pantosx, J. K. M. Sanders, M. Orlandi, C. Chiorboli, S. Fracassio and F. Scandola, *Chem. Sci.*, 2011, **2**, 676.
- 8 (a) K. Konishi, K. Makita, T. Aida and S. Inoue, *J. Chem. Soc., Chem. Commun.*, 1988, 643; (b) Y. Sato, T. Arai and S. Inoue, *Chem. Lett.*, 1990, 551; (c) M. Komatsu and T. Aida, *J. Am. Chem. Soc.*, 1991, **113**, 8492; (d) T. Aida, H. Sugimoto, M. Kuroki and S. Inoue, *J. Phys. Org. Chem.*, 1995, **8**, 249.
- 9 Y. Kaizu, N. Misu, K. Tsuji, Y. Kaneko and H. Kobayashi, *Bull. Chem. Soc. Jpn.*, 1985, **58**, 103.
- 10 (a) L. Latos-Grazynski, in *The Porphyrin Handbook*, ed. K. M. Kadish, K. M. Smith and R. Guilard, Academic Press, New York, 2000, vol. 2, p. 361; (b) I. Gupta and M. Ravikanth, *Coord. Chem. Rev.*, 2006, **250**, 468; (c) M. Yedukondalu and M. Ravikanth, *Coord. Chem. Rev.*, 2011, **255**, 547.
- 11 (a) T. K. Chandrashekar and S. Venkatraman, *Acc. Chem. Res.*, 2003, **36**, 676; (b) R. Misra and T. K. Chandrashekar, *Acc. Chem. Res.*, 2008, **41**, 265.
- 12 (a) V. S. Shetti and M. Ravikanth, *Inorg. Chem.*, 2010, **49**, 2692; (b) V. S. Shetti and M. Ravikanth, *Inorg. Chem.*, 2011, **50**, 1713.
- 13 I. Gupta and M. Ravikanth, *Inorg. Chim. Acta*, 2007, **360**, 1731.
- 14 M. W. Schmidt, K. K. Baldrige, J. A. Boatz, S. T. Elbert, M. S. Gordon, J. H. Jensen, S. Koseki, N. Matsunaga, K. A. Nguyen, S. J. Su, T. L. Windus, M. Dupuis and J. A. Montgomery, *J. Comput. Chem.*, 1993, **14**, 1347.
- 15 G. Schaftenaar and J. H. Noordik, *J. Comput.-Aided Mol. Des.*, 2000, **14**, 123.